Robust Heart Rate Estimation using Wrist-based PPG Signals in the Presence of Intense Physical Activities

Chengzhi Zong, *Student Member*, *IEEE,* Roozbeh Jafari, *Senior Member, IEEE*

***Abstract*— Heart rate tracking from a wrist-type photoplethysmogram (PPG) signal during intensive physical activities is a challenge that is attracting more attention thanks to the introduction of wrist-worn wearable computers. Commonly-used motion artifact rejection methods coupled with simple periodicity-based heart rate estimation techniques are incapable of achieving satisfactory heart rate tracking performance during intense activities. In this paper, we propose a two-stage solution. Firstly, we introduce an improved spectral subtraction method to reject the spectral components of motion artifacts. Secondly, instead of using heuristic mechanisms, we formalize the spectral peaks selection process as the shortest path search problem and validate its effectiveness. Analysis on the experimental results based on a published database shows that: (1) Our proposed method outperforms three other comparable methods with regards to heart rate estimation error. (2) The proposed method is a promising candidate for both offline cardiac health analysis and online heart rate tracking in daily life, even during intensive physical motions.**

I. Introduction

With the rapid enhancement in electronics technology miniaturization, ubiquitous monitoring of human health and well-being is gaining more attention leveraging wearable computers. This trend has resulted in the emergence of the wearable healthcare devices. Among all vital signs to monitor, cardiac activity is always regarded as one with great importance. One public health report in 2010 showed that almost 1 in every 4 deaths is due to heart diseases every year in the United States [1]. One straightforward indicator of heart health is the heart beat rate, the monitoring of which alone could assist clinical experts to diagnose or predict certain heart diseases at an early stage [2] or intuitively inform the user his or her heart health status. The community has recently observed the emerging approach of incorporating this monitoring functionality into so-called *smart watches*, *e.g.*, Samsung's Gear series, Motorola's Moto 360, etc. It is common among most of these commercial products that the heart rate is estimated based on the photoplethysmogram (PPG) signal collected from a wrist-worn pulse oximeter embedded inside the watch. However, this wrist-worn monitor makes heart beat tracking highly sensitive and vulnerable to human physical motions. Therefore to decode the heart health status more reliably, which in this context implies more accurate heart rate estimation, the artifacts introduced by the physical motions, termed as *motion artifacts*, need to be extracted and rejected from the original noisy PPG signal.

Chengzhi Zong is a Ph.D. student of Electrical Engineering in University of Texas at Dallas, Richardson, Texas, 75080 USA. (phone: 352-665-0384; e-mail: cxz121430@utdallas.edu).

Roozbeh Jafari is an associate professor of Electrical Engineering in University of Texas at Dallas, Richardson, Texas, 75080 USA. (e-mail: rjafari@utdallas.edu).

Therefore, the task of estimating heart rate from highly-corrupted PPG signal could be divided into two sub-problems: motion artifact rejection and heart rate frequency estimation. Neither of them is a trivial problem since: (1) the frequency band for heart rate, ranging from 1Hz to 4Hz, overlaps with that of the motion artifact, which ranges from 0.1-20Hz [3]. Thus, common filtering cannot always remove the motion artifact effectively. (2) The signal-to-noise ratio (SNR) of the PPG signal collected during motion is very low, and gets much worse during intensive physical motion. Therefore, simple pitch detection algorithms that have been successful in other instances with moderate SNR will not be suitable for wrist-worn PPG-based heart rate estimation.

Numerous investigations have been devoted to these two sub-problems. For the former, efforts are concentrated on attenuating motion artifacts and enhancing the SNR. Adaptive filtering is applied to weaken the motion artifact with the aid of other signals that correlate well only with the motions but not with the PPG signal [3-6]. These are termed as 'motion artifact-correlated signals'. Different adaptive algorithms, such as recursive least squares (RLS) [3], normalized least mean squares (NLMS) [3-4] and variable step-size least mean squares [5] have been implemented along with different motion artifact-correlated signals: optoelectronic sensor [3,5], accelerometer [4] and synthetic reference signals [6]. However, the performance of these adaptive filtering methods has only been tested in experiments where the pulse oximeters are placed on the fingertip, which enhances the SNR and reduces the sensitivity of the collected PPG signals to the physical motions. Apart from adaptive filters independent component analysis (ICA), a popular realization of blind source separation (BSS), is used to separate the clean PPG signal from motion artifacts [7]. Nevertheless, the assumption that the PPG signal and motion artifacts are statistically independent from each other does not always hold [8]. Another alternative for PPG de-noising is spectral subtraction [9]. This method estimates the frequency spectrum of motion artifacts according to the motion artifact-correlated signal and subtract it from the frequency spectrum of the original noisy PPG signal. However, we observed in our experiments that the correlation between motion artifacts and the motion artifact-correlated signals is not consistently high, hence a simple subtraction operation does not always work well for two signals collected from different systems—pulse oximeter and accelerometer. In this paper, we improve the original spectral subtraction method by addressing these defects. The proposed method mainly consists of three parts: *spectrogram normalization*, *subtraction conditioning* and *spectrogram masking*.

Several techniques have been proposed for heart rate frequency estimation during physical motions. Several popular algorithms, *e.g.*, autocorrelation-based algorithms

978-1-4244-9270-1/15/$31.00 ©2015 IEEE

and harmonic product spectrum (HPS) have been employed successfully for similar purposes in speech recognition and other topics, but the periodicity quickly vanishes in low-SNR PPG signals acquired from the wrist, thus using these algorithms alone is not sufficient to obtain satisfactory performance. One work has recently proposed sparse signal reconstruction (SSR) instead of discrete Fourier transform (DFT) to enhance the performance of spectrum estimation [10], followed by another process for choosing the heart rate from various peaks of the power spectral density (PSD). However, to the best of our knowledge, this so-called spectral peaks search process is usually realized with different heuristic rules and techniques and are not very reliable [10-11]. In this paper, instead of designing a heuristic method, we formalize this spectral peaks search problem to be a directed, single-pair shortest path search problem, and the heart rate frequencies will be discovered when the shortest path is determined.

The main contribution of our work towards heart rate estimation during intensive physical motion is two-fold:

- We propose an improved spectral subtraction method to address the defects of current approaches for the motion artifact rejection in PPG signal.
- We formalize the spectral peaks search process as a shortest path search problem to improve the heart rate estimation performance and provide a systematic guidance for future related work.

II. Proposed Method

As outlined in previous section, our proposed method is comprised of two parts: motion artifact rejection and heart rate frequency estimation.

A. Motion Artifact Rejection

For the motion artifact rejection, firstly, short-time Fourier transform (STFT) is applied to obtain the spectrogram of the original PPG signal, as shown in (1) and (2), where the Hamming window is chosen to be the window function $w[n]$.

$$STFT\{x[n]\}(t,\omega) = \sum_{n=-\infty}^{\infty} x[n]w[n-t]\,e^{-j\omega n} \quad (1)$$

$$spectro\{x[n]\}(t,\omega) = |STFT\{x[n]\}(t,\omega)|^2 \quad (2)$$

We denote the clean PPG signal, the motion artifact coupled with the clean PPG and the motion artifact-correlated signal as $s[n]$, $m[n]$ and $\hat{m}[n]$, respectively. We essentially model our acquired noisy PPG signal with $x[n] = s[n] + m[n]$. Since motion artifact-related signal $\hat{m}[n]$ correlates with the motion artifact $m[n]$, subtracting the power spectrum of $\hat{m}[n]$, denoted as $spectro\{\hat{m}[n]\}$ from the power spectrum of noisy PPG signal ($s[n] + m[n]$), denoted as $spectro\{s[n] + m[n]\}$ would seemingly reduce the influence of the motion artifact. However, because signals $s[n] + m[n]$ (noisy PPG) and $\hat{m}[n]$ (motion-artifact correlated signal) are collected from two separate systems, the unit and the amplitude of these two types of signals are unlike and a normalization process is required. One more issue is that the power spectrum of $s[n]$ may overlap with that of $m[n]$ in certain situations, that is the principal frequencies of the heart rate and motions become identical. Therefore, the subtraction needs to be conditional; that is, it should only be applied when the heart rate frequency differs from the frequency of physical motions. We will explain this in Subsection II.2. As shown in the flowchart in Fig. 1, *spectrogram normalization* and *subtraction conditioning* function blocks are designed to solve these two sub-problems, respectively, followed by the last function block *spectrogram masking*.

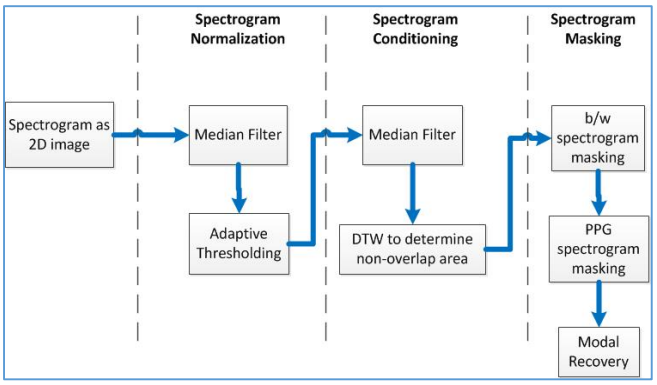

Figure 1. Flowchart of the motion artifact rejection

1) Spectrogram Normalization: The spectrogram of PPG signal could be regarded as a 2-D grayscale image. For further inter-operation between $spectro\{\hat{m}[n]\}$ and $spectro\{s[n] + m[n]\}$, normalization is performed by binarizing this grayscale image.

a) Median Filter: A 2-D median filter is used to remove the so-called 'salt-and-pepper noise' while smoothing the edges for the following thresholding process [12].

b) Adaptive Thresholding: Thresholding process is needed here to unify dissimilar units and amplitudes from two measurement systems, that is, the system used to collect PPG signals and the system used to collect motion artifact-correlated signals (accelerometer sensors). $spectro\{\hat{m}[n]\}$ and $spectro\{s[n] + m[n]\}$ are normalized by performing an adaptive thresholding. The reason for using an adaptive threshold rather than a global threshold for our problem is that the intensity of motion randomly changes over time; so using a fixed global threshold throughout the entire time range may lead to missing certain important heart rate information or retaining unnecessary noise. Therefore, an adaptive threshold is more suitable. In our work, Otsu's method, a clustering-based image thresholding algorithm is applied [13]. The optimal threshold Th_{opt}^t at time instance t could be determined by minimizing the overall within-class variance as shown in (3):

$$Th_{opt}^t = \underset{Th^t}{\operatorname{argmin}}[n_B(Th^t)\sigma_B^2(Th^t) + n_F(Th^t)\sigma_F^2(Th^t)] \quad (3)$$

Where $n_B(Th^t)$ and $n_F(Th^t)$ are percentage of pixels in background and foreground respectively, and $\sigma_B^2(Th^t)$ and $\sigma_F^2(Th^t)$ are the variance of the pixels in the background and foreground. To satisfy the premise of the Otsu's method that the intensity of pixels are bi-normally distributed, we choose the operation region to be the power spectral density (PSD) at each time instance, *i.e.*, vertical lines in the spectrogram.

As shown in (4), the binary spectrogram $\overline{spectro}\{x[n]\}(t,\omega)$ is then obtained by thresholding based on the Th_{opt}^{t} for every time instance t.

$$\overline{spectro}\{x[n]\}(t,\omega) = \begin{cases} 1, spectro\{x[n]\}(t,\omega) \geq Th_{opt}^{t} \\ 0 \quad\quad\quad\quad\quad\quad others \end{cases} \quad (4)$$

2) Subtraction Conditioning: An unconditional subtraction process on the spectrogram may result in depletion of heart rate information, especially when the heart rate frequency overlaps with that of the motion artifact. Therefore, after going through another median filter to smooth out the noise generated by the thresholding, the resultant binary spectrogram $\overline{spectro}\{x[n]\}(t,\omega)$ needs to be separated into different regions and only the regions where overlapping does not exist could be included in spectral subtraction. We also observe that the PSD of the PPG signal and that of the motion artifact-correlated signal could maintain similar patterns and the principal components may overlap. A similarity measure would be able to determine the existence of the overlapping and accordingly perform the conditional spectral subtraction. However, it's observed that the motion artifact in PPG signal and the additional motion artifact-correlated signal do not always perfectly correlate with each other. That is, the pattern of the PSD of noisy PPG signal and that of the additional motion artifact-correlated signal may look similar but have peaks' locations shifted, which might be due to slight displacement and tightness of the PPG sensor and motion sensor. To address this issue, dynamic time warping (DTW) [14] is adopted to measure the inherent similarity regardless of the peaks shift. Thereafter, the boundary of the area where spectral subtraction is required is determined.

3) Spectrogram Masking: Inside the area deteremined through *Subtraction conitioning*, denoted as A_{sub}, the binary spectrogram of the motion artifact-correlated signal $\overline{spectro}\{\hat{m}[n]\}$ is subtracted from the binary spectrogram of the PPG signal $\overline{spectro}\{s[n]+m[n]\}$ to cancel out the motion artifact (for simplicity, $\overline{spectro}\{x[n]\}$ is used instead of $\overline{spectro}\{x[n]\}(t,\omega)$ and the same applies to the rest of the terms). Outside A_{sub}, $\overline{spectro}\{s[n]+m[n]\}$ remains unchanged. This process is shown in Eq. (5). Afterwards, the resultant binary spectrogram $\overline{\overline{spectro}}\{s[n]+m[n]\}$ is used as masking to denoise the original PPG signal's spectrogram $spectro\{x[n]\}$ by retaining only the pixels that have value '1' in $\overline{\overline{spectro}}\{s[n]+m[n]\}$, shown in Eq. (6).

$$\overline{\overline{spectro}}\{s[n]+m[n]\} = \begin{cases} \overline{spectro}\{s[n]+m[n]\} - \overline{spectro}\{\hat{m}[n]\} & , in\ A_{sub} \\ \overline{spectro}\{s[n]+m[n]\} & , outside\ A_{sub} \end{cases} \quad (5)$$

$$\widehat{spectro}\{s[n]+m[n]\} = \begin{cases} spectro\{x[n]\} & , \overline{\overline{spectro}}\{s[n]+m[n]\} == 1 \\ 0 & , others \end{cases} \quad (6)$$

B. Heart Rate Frequency Estimation

The heart rate frequency estimation is then applied based on the refined spectrogram of the PPG signal with enhanced SNR, *i.e.*, $\widehat{spectro}\{s[n]+m[n]\}$. Nevertheless, even if after the de-noising process, the frequencies appearing as peaks in the PSD would all be considered as candidates for the heart rate frequencies. Therefore a follow-up processing, termed spectral peaks tracking is required. However, to the best of our knowledge, most implementations for this process is composed of various heuristic rules [10-11]. In our work, inspired by the fact that in normal condition, heart rate variation is small during short time interval, *e.g.*, within 2 second, we believe the estimation of a sequence of heart rate frequencies will outperform methods that are based on a single instantaneous heart rate alone. Also, considering only one of all the heart rate candidates at any time (multiple candidates may exists due to the motion artifacts) is valid and the heart rate frequency estimation could indeed be formulated as a directed, single-pair shortest path search problem.

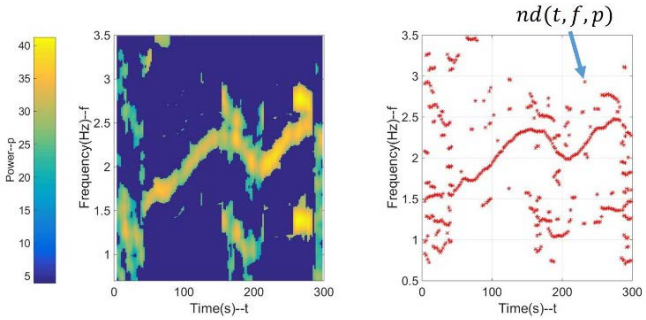

Figure 2. Candidate set for heart rate frequencies

In the refined spectrogram $\widehat{spectro}\{s[n]+m[n]\}$, the frequencies with peaks in the PSD are regarded as the candidates of the true heart rate, all of which form a candidate set over time, as shown in Fig. 2. Each candidate node $nd(t,f,p)$ inside is represented by time t, frequency f and power p at that frequency. In Fig. 2, the x axis is time t, y axis represents frequency f and z axis represents power p of frequency f represented by a color spectrum. We take advantage of the facts that (1) the variations in heart rate in a short time window is limited and (2) the power of heart rate frequency should be higher than most other frequencies in the spectrogram of the resultant refined PPG. We design a cost function for each pair of time-neighbored candidate nodes, and the sequence of heart rate frequencies is discovered by a backward shortest path search. It is important to note that only one node $nd(t,f,p)$ could be selected for any specific time t and the time is always moving forward.

Algorithm I. Design of cost function and backward shortest path search for heart rate frequencies sequence.

- The lower and upper bound of valid heart rate frequency is f_{low} and f_{up}, with resolution Δf and total step number N_f.
- The starting and ending time of path search is t_{init} and t_{end}, with step Δt and total step number N_t.
- p_t^f represents the power p at frequency f of the candidate node $nd(t,f,p)$ at time t.
- $t = t_{init}:\Delta t:t_{end}$
  $P(t)$={$p_t^{f_c} | p_t^{f_c}$ is a local maxima in power spectral density among $p_t^{f_{low}} \ldots p_t^{f_{up}}$}
  $F(t)$={all f_c at time t}
  $n(t)$={total number of f_c at time t}
  end
- j_t is the index of candidate nodes at time t, $j_t \in [1,\ldots,n(t)]$

- $f_t^{j_t}$ and $p_t^{j_t}$ are the frequency and power of the j_t th candidate node at time *t, and* $f_t^{j_t} \in F(t)$, $p_t^{j_t} \in P(t)$. To simplify the notation, we use f_t^j for $f_t^{j_t}$ and p_t^j for $p_t^{j_t}$.
- Cost function $d_{\Delta t}^{jk}$ between the j^{th} candidate node at time t and the k^{th} candidate node at time $t-\Delta t$ is designed as:

$$d_{\Delta t}^{jk} = \frac{\exp\left|coef*\left(f_t^j - f_{t-\Delta t}^k\right)\right|}{p_t^j p_{t-\Delta t}^k}, \quad j \in n(t),\ k \in n(t-\Delta t) \tag{7}$$

  Where $f_t^j - f_{t-\Delta t}^k$ in numerator and $p_t^j p_{t-\Delta t}^k$ in denominator makes the algorithm tend to select the candidate nodes having smaller frequency variation from the time-neighbored nodes and higher power. Moreover, exponential function introduces non-linear penalty to higher frequency variation, and parameter $coef$ tunes the contribution from these two aspects.
- $D_t^{j_t}$ is the accumulated distance of the j_t th candidate node at time *t,* we use D_t^j for $D_t^{j_t}$.

$$D_t^j = \min_k (D_{t-\Delta t}^k + d_{\Delta t}^{jk}) \tag{8}$$

$$Prev_t^j = arg\min_k \left(D_{t-\Delta t}^k + d_{\Delta t}^{jk}\right) \tag{9}$$

  with $j \in n(t),\ k \in n(t-\Delta t)$.
- $Index_t$ is the index of selected node at time *t.*
  Find the minimal accumulated distance at t_{end}:

$$Index_{t_{end}} = arg\min_j D_{t_{end}}^j \quad , j \in n(t_{end}) \tag{10}$$

$$j_{curr} = Index_{end} \tag{11}$$

- Backward search for the index of the heart rate frequencies:
  $t = t_{end} - \Delta t : \Delta t : t_{init}$

$$Index_t = Prev_t^{j_{curr}} \tag{12}$$

$$j_{curr} = Index_t \tag{13}$$

  end

Therefore, this is a directed and single-pair shortest path problem. The detailed design of the cost function and backward shortest path search for the sequence of heart rate frequencies are described in Algorithm I.

III. Experimental Results

A. Experimental Setup

We validated our method on a published database of IEEE Signal Processing Cup 2015 [10]. There are 12 subjects aged from 18 to 35 included in this database. The dataset of each subject consists of two-channel PPG signals, three-axis acceleration signals and one-channel ECG signal. Two pulse oximeters with green LEDs are used with placement 2-cm apart, and embedded together with the accelerometer in a wrist-worn device. The ECG signal was recorded simultaneously from the chest using wet ECG sensors to be used as the ground truth, and the acceleration signals are used as motion artifact-correlated signals. All signals were sampled at 125Hz and sent to a nearby computer via Bluetooth. The following two physical exercises scenarios are considered, and the speed of running is controlled by a treadmill:

1. rest(30s) -> 8km/h(1min) -> 15km/h(1min) -> 8km/h(1min) -> 15km/h(1min) -> rest(30s)
2. rest(30s) -> 6km/h(1min) -> 12km/h(1min) -> 6km/h(1min) -> 12km/h(1min) -> rest(30s)

B. Results

In Fig.3, one illustrative example for subject 2 is demonstrated to show the effectiveness of the proposed motion artifact rejection method. The top two sub-figures reflects and validates the high correlation in power spectrum between the acceleration signal and the motion artifact in the PPG signal. A similar pattern shown in the bottom two sub-figures indicates that the proposed three-stage motion artifact rejection method could indeed enhance the signal-to-noise ratio of the PPG signal.

We validated the performance of our proposed method for heart rate frequency estimation. In Table I, the average error of the estimation during a period of 5 minutes is listed for all 12 subjects, in units of beats per minute (BPM). We compared our approach to the the NLMS-based [3], ICA-based [7] and the TROIKA [10] tracking algorithms. We observed that the adaptive filtering-based and ICA-based algorithms are not able to obtain acceptable performance during these intensive physical motions, although they are reported to perform well in situations of mild physical motion, especially with fingertip-based pulse oximeters. The reasons could be (1) the correlation between the acceleration

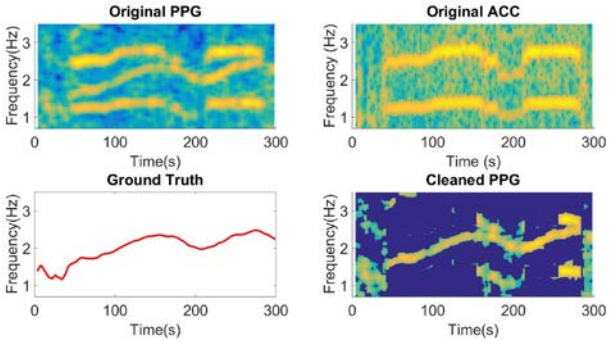

Figure 3. Spectrogram of original PPG signal (top left), spectrogram of original acceleration signal (top right), ground truth of heart rate frequency over time (bottom left), spectrogram of refined PPG signal (bottom right) – for subject 2

Table I. Comparison of the estimation error between the proposed method and other works on 12 subjects (unit: beats/minute)

Error (bpm) \ Subject	1	2	3	4	5	6	7	8	9	10	11	12	average
NLMS adaptive filter [3]	22.8	36.4	35.1	21.1	8.61	19.4	12.3	20.2	18.7	12.7	8.28	26.3	20.2
ICA [7]	19.3	25.2	24.3	16.1	9.56	25.5	7.11	18.0	15.5	25.7	9.37	23.3	18.2
TROIKA [10]	2.29	2.19	2.00	2.15	2.01	2.76	1.67	1.93	1.86	4.70	1.72	2.84	2.34
Our proposed method	1.05	0.98	1.26	1.33	0.66	0.77	0.41	0.47	0.35	3.49	0.50	1.52	1.07

signals and the motion artifacts are not always significant in the presence of intensive motion, which invalidates the usage of adaptive filter. (2) When the user performs intensive motion, the heart rate is more likely to be influenced by the degree of the intensity of the motion, thus nullifying the ICA's assumption on the statistical independence between these two signals. Furthermore, our method outperforms the TROIKA, which employed well-designed but heuristic rules for the spectral peaks search.

We evaluated the effectiveness of our algorithm and compared the estimated and the true heart rate. The correlation plot and the Bland-Altman plot on the 12 datasets are shown in Fig.4 (a) and (b), respectively. The corresponding Pearson correlation coefficient is 0.995, and the 95% limits of agreement is [-4.4, 5.4] BPM.

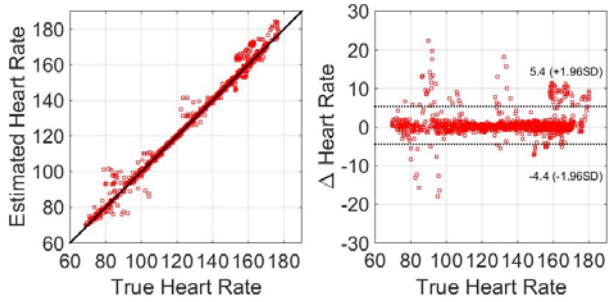

(a) Correlation (b) Bland-Altman plot

Figure 4. Agreement between estimated and true heart rate

IV. CONCLUSION

In this paper, we proposed a novel method to track the heart rate using PPG signals acquired from a wrist-worn device during intensive physical motions. The proposed method consists of a spectrum-based motion artifact rejection technique and a formalized spectral peaks tracking algorithm. The experimental results indicate that our algorithm has superior tracking performance compared to three other widely used or recently proposed algorithms. Moreover, the analysis comparing the estimation to the ground truth as well as the analysis on the real-time implementation imply a promising future commercial usage.

ACKNOWLEDGEMENT

This work was supported in part by the National Science Foundation, under grant CNS-1150079. Any opinions, findings, conclusions, or recommendations expressed in this material are those of the authors and do not necessarily reflect the views of the funding organizations.

REFERENCES

1. Murphy SL, Xu JQ, Kochanek KD. Deaths: Final data for 2010. Natl Vital Stat Rep. 2013; 61(4).
2. M. Chessa, G. Butera, G. A. Lanza, E. Bossone, A. Delogu, G. De Rosa, G. Marietti, L. Rosti, and M. Carminati, "Role of heart rate variability in the early diagnosis of diabetic autonomic neuropathy in children," Herz, vol. 27, no. 8, pp. 785–790, 2002.
3. Shimazaki, T.; Hara, S.; Okuhata, H.; Nakamura, H.; Kawabata, T., "Cancellation of motion artifact induced by exercise for PPG-based heart rate sensing," Engineering in Medicine and Biology Society (EMBC), 2014 36th Annual International Conference of the IEEE , vol., no., pp.3216,3219, 26-30 Aug. 2014
4. Hyonyoung Han; Min-Joon Kim; Jung Kim, "Development of real-time motion artifact reduction algorithm for a wearable photoplethysmography," Engineering in Medicine and Biology Society, 2007. EMBS 2007. 29th Annual International Conference of the IEEE , vol., no., pp.1538,1541, 22-26 Aug. 2007
5. Chan, K.W.; Zhang, Y.T., "Adaptive reduction of motion artifact from photoplethysmographic recordings using a variable step-size LMS filter," Sensors, 2002. Proceedings of IEEE , vol.2, no., pp.1343,1346 vol.2, 2002
6. Yousefi, R.; Nourani, M.; Ostadabbas, S.; Panahi, I., "A Motion-Tolerant Adaptive Algorithm for Wearable Photoplethysmographic Biosensors," Biomedical and Health Informatics, IEEE Journal of , vol.18, no.2, pp.670,681, March 2014
7. Kim, B.S.; Yoo, S.K., "Motion artifact reduction in photoplethysmography using independent component analysis," Biomedical Engineering, IEEE Transactions on , vol.53, no.3, pp.566,568, March 2006
8. Yao, J.; Warren, S., "A Short Study to Assess the Potential of Independent Component Analysis for Motion Artifact Separation in Wearable Pulse Oximeter Signals," Engineering in Medicine and Biology Society, 2005. IEEE-EMBS 2005. 27th Annual International Conference of the , vol., no., pp.3585,3588, 2005
9. Fukushima, H.; Kawanaka, H.; Bhuiyan, M.S.; Oguri, K., "Estimating heart rate using wrist-type Photoplethysmography and acceleration sensor while running," Engineering in Medicine and Biology Society (EMBC), 2012 Annual International Conference of the IEEE , vol., no., pp.2901,2904, Aug. 28 2012-Sept. 1 2012
10. Zhang, Z.; Pi, Z.; Liu, B., "TROIKA: A General Framework for Heart Rate Monitoring Using Wrist-Type Photoplethysmographic (PPG) Signals During Intensive Physical Exercise," Biomedical Engineering, IEEE Transactions on , vol.PP, no.99, pp.1,1
11. López, Sonia María, et al. "Heuristic algorithm for photoplethysmographic heart rate tracking during maximal exercise test." (2012).
12. Huang, T., G. Yang, and G. Tang. "A fast two-dimensional median filtering algorithm." Acoustics, Speech and Signal Processing, IEEE Transactions on27.1 (1979): 13-18.
13. Otsu, Nobuyuki. "A threshold selection method from gray-level histograms."Automatica 11.285-296 (1975): 23-27.
14. Senin, Pavel. "Dynamic time warping algorithm review." Information and Computer Science Department University of Hawaii at Manoa Honolulu, USA(2008): 1-23.